

(2)

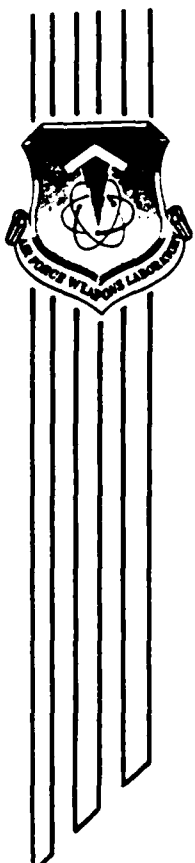
DTIC FILED

AD-A193 902

FREQUENCY DOUBLING AT 1.315  $\mu$ m

R. H. Humphreys  
D. E. Johnson  
P. Keating  
G. D. Hager

February 1988



Final Report

Approved for public release; distribution unlimited.

AIR FORCE WEAPONS LABORATORY  
Air Force Systems Command  
Kirtland Air Force Base, NM 87117-6008

DTIC  
SELECTED  
APR 27 1988  
S E D

This final report was prepared by the Air Force Weapons Laboratory, Kirtland Air Force Base, New Mexico, Job Order ILIR8406. Capt Daniel E. Johnson (ARBI) was the Laboratory Project Officer-in-Charge.

When Government drawings, specifications, or other data are used for any purpose other than in connection with a definitely Government-related procurement, the United States Government incurs no responsibility or any obligation whatsoever. The fact that the Government may have formulated or in any way supplied the said drawings, specifications, or other data, is not to be regarded by implication, or otherwise in any manner construed, as licensing the holder, or any other person or corporation; or as conveying any rights or permission to manufacture, use, or sell any patented invention that may in any way be related thereto.

This report has been authored by employees of the United States Government. Accordingly, the United States Government retains a nonexclusive, royalty-free license to publish or reproduce the material contained herein, or allow others to do so, for the United States Government purposes.

This report has been reviewed by the Public Affairs Office and is releasable to the National Technical Information Service (NTIS). At NTIS, it will be available to the general public, including foreign nationals.

If your address has changed, if you wish to be removed from our mailing list, or if your organization no longer employs the addressee, please notify AFWL/ARBI, Kirtland Air Force Base, NM 87117-6008 to help us maintain a current mailing list.

This report has been reviewed and is approved for publication.

*Daniel E Johnson*  
DANIEL E. JOHNSON  
Captain, USAF  
Project Officer

*Gerald A. Hasen*  
GERALD A. HASEN  
Major, USAF  
Ch, Advanced Chemical Laser Branch

FOR THE COMMANDER

*Harr. Ackermann*  
HARRO ACKERMANN  
Lieutenant Colonel, USAF  
Ch, Laser Science and Technology Office

DO NOT RETURN COPIES OF THIS REPORT UNLESS CONTRACTUAL OBLIGATIONS OR NOTICE ON A SPECIFIC DOCUMENT REQUIRES THAT IT BE RETURNED.

UNCLASSIFIED

SECURITY CLASSIFICATION OF THIS PAGE

## REPORT DOCUMENTATION PAGE

1a. REPORT SECURITY CLASSIFICATION Unclassified		1b. RESTRICTIVE MARKINGS			
2a. SECURITY CLASSIFICATION AUTHORITY		3. DISTRIBUTION/AVAILABILITY OF REPORT Approved for public release; distribution unlimited.			
2b. DECLASSIFICATION / DOWNGRADING SCHEDULE					
4. PERFORMING ORGANIZATION REPORT NUMBER(S) AFWL-TR-87-54		5. MONITORING ORGANIZATION REPORT NUMBER(S)			
6a. NAME OF PERFORMING ORGANIZATION Air Force Weapons Laboratory	6b. OFFICE SYMBOL (if applicable) ARBI	7a. NAME OF MONITORING ORGANIZATION			
6c. ADDRESS (City, State, and ZIP Code) Kirtland AFB, New Mexico 87117-6008		7b. ADDRESS (City, State, and ZIP Code)			
8a. NAME OF FUNDING/SPONSORING ORGANIZATION	8b. OFFICE SYMBOL (if applicable)	9. PROCUREMENT INSTRUMENT IDENTIFICATION NUMBER			
8c. ADDRESS (City, State, and ZIP Code)		10. SOURCE OF FUNDING NUMBERS			
		PROGRAM ELEMENT NO 62601F	PROJECT NO ILIR	TASK NO 84	WORK UNIT ACCESSION NO 06
11. TITLE (Include Security Classification) FREQUENCY DOUBLING AT 1.315 $\mu$ m					
12. PERSONAL AUTHOR(S) Humphreys, R. H.; Johnson, D. E.; Keating, P.; and Hager, G. D.					
13a. TYPE OF REPORT Final	13b. TIME COVERED FROM Sep 84 to Aug 85	14. DATE OF REPORT (Year, Month, Day) 1988, February		15. PAGE COUNT 28	
16. SUPPLEMENTARY NOTATION					
17. COSATI CODES		18. SUBJECT TERMS (Continue on reverse if necessary and identify by block number) Frequency doubling, Second harmonic generation, Intra-cavity, Extracavity, Lithium iodate, Chemical oxygen iodine laser, Photolytic iodine laser.			
19. ABSTRACT (Continue on reverse if necessary and identify by block number) Using lithium iodate crystals, second harmonic generation of chemical oxygen iodine laser (COIL) light ( $\lambda = 1.315 \mu$ m) has been demonstrated for the first time. Both a photolytic iodine laser and a COIL were used. For the photolytic iodine laser, 320 mW of red output in 40 $\mu$ s pulses was generated in an extracavity configuration at a conversion efficiency of $2.1 \times 10^{-5}$ . With the COIL device, 60 mW of average second harmonic power was observed at an overall conversion efficiency of 1 percent when the crystal was placed intracavity. In both cases, experimental second harmonic powers were in good agreement with theoretical values.					
20. DISTRIBUTION/AVAILABILITY OF ABSTRACT <input type="checkbox"/> UNCLASSIFIED/UNLIMITED <input checked="" type="checkbox"/> SAME AS RPT <input type="checkbox"/> DTIC USERS		21. ABSTRACT SECURITY CLASSIFICATION Unclassified			
22a. NAME OF RESPONSIBLE INDIVIDUAL Capt Daniel E. Johnson		22b. TELEPHONE (Include Area Code) (505) 844-0662	22c. OFFICE SYMBOL AFWL/ARBI		

DD FORM 1473, 84 MAR

83 APR edition may be used until exhausted

All other editions are obsolete

SECURITY CLASSIFICATION OF THIS PAGE

UNCLASSIFIED

UNCLASSIFIED

SECURITY CLASSIFICATION OF THIS PAGE

UNCLASSIFIED

SECURITY CLASSIFICATION OF THIS PAGE

## CONTENTS

<u>Section</u>		<u>Page</u>
1.0	INTRODUCTION	1
2.0	THEORY	3
3.0	EXPERIMENTAL RESULTS	7
	3.1 Z-PINCH LASER	7
	3.2 Recoil LASER	9
4.0	CONCLUSIONS	13

<u>Accession For</u>	
NTIS GRA&I	<input checked="" type="checkbox"/>
DTIC TAB	<input type="checkbox"/>
Unannounced	<input type="checkbox"/>
<u>Justification</u>	
By _____	
<u>Distribution/</u>	
<u>Availability Codes</u>	
Dist	Avail and/or Special
A-1	



## 1.0 INTRODUCTION

Optical second harmonic generation (SHG) is a way in which the Chemical Oxygen-Iodine Laser (COIL) can be used to produce visible wavelengths. The COIL is an inherently scalable, high energy storage laser operating on the  $I(^2P_{1/2}) \rightarrow I(^2P_{3/2})$  transition ( $\lambda = 1.315 \mu\text{m}$ ). By converting the COIL output from the infrared (IR) to the red ( $\lambda/2 = 658 \text{ nm}$ ), one would have the advantages of an IR laser in terms of optical materials and ease of lasing, and the advantages of a visible laser in terms of lower intrinsic beam divergence, higher brightness and better target interaction. An efficient, compact visible chemical laser, therefore, would be available.

Second harmonic generation was first demonstrated in 1961 (Ref. 1), with roughly 60 nJ of second harmonic power being produced from a 3 J ruby laser ( $\lambda = 694 \text{ nm}$ ). Since then, more powerful lasers, better quality crystals and optics, and more refined experimental techniques have increased conversion efficiencies greatly. In its simplest form, SHG is performed with the SHG medium, usually a birefringent crystal, external to the laser resonator (extracavity). Because of the high fluxes required for efficient extracavity conversion, SHG is generally performed with extremely high power, short pulse lasers such as Nova and Argus (Nd: Glass) at Lawrence Livermore National Laboratory (Ref. 2) and the Asterix (Iodine) devices at the Max Planck Institut für Quantenoptik (Ref. 3). These fusion drivers, capable of generating intensities in excess of  $\text{GW/cm}^2$ , have produced SHG conversion efficiencies of 30 percent, and have even generated the sixth harmonic.

The situation for continuous wave (CW) lasers such as the COIL is different. Even for high average power devices, single pass conversion efficiencies are on the order of a hundredth of a percent. One way to alleviate the problem of low single pass conversion efficiency is to place the SHG crystal inside the resonator (intracavity), thereby forcing the fundamental beam to pass through the crystal several times before it is outcoupled. In its purest form, intracavity doubling is performed with a stable resonator in which both mirrors are 100 percent reflecting at the fundamental; one of the mirrors is 100 percent reflecting at the second harmonic and the other 100 percent transmitting at the

second harmonic. In theory, even with a low average power CW laser, 100 percent conversion efficiency should be obtainable in this configuration in the limit of no internal losses (Ref. 4). Experimentally, it has been shown (Ref. 5) that all the fundamental power produced with the crystal inserted intracavity was converted to the second harmonic. In an intracavity configuration, crystal absorption is extremely critical because of the large number of passes the fundamental beam makes through the crystal. If the crystal absorption is too high, a number of problems can result: the crystal can heat and go off phase match or even crack due to thermal stresses, and the power output of the laser at the fundamental can drop severely, or lasing can even cease in a low gain laser such as COIL.

The SHG of COIL laser light is reported here for the first time. A pulsed photolytic iodine laser was used in extracavity doubling experiments and a CW COIL device was used in intracavity experiments. In both cases, lithium iodate crystals were used as the frequency doubler.

## 2.0 THEORY

Second harmonic generation is a specialized case of the nonlinear process of three wave mixing in which the two pump waves have identical frequency. A thorough treatment of the subject is presented in Refs. 6 through 8. A brief description begins with Maxwell's equations for a polarizable material:

$$\nabla \times \nabla \times \vec{E} + \mu \epsilon \frac{\partial^2 \vec{E}}{\partial t^2} + \mu \frac{\partial^2 \vec{P}}{\partial t^2} = 0 \quad (1)$$

where  $\vec{E}$  = electric field vector

$\epsilon$  = permittivity of the medium

$\mu$  = permeability of the medium

$\vec{P}$  = nonlinear charge polarization

Assuming propagation in the + Z direction and slowly varying field amplitude in the Z direction, the governing equations can be simplified to:

$$\frac{dE_1(Z)}{dZ} = \frac{-i\omega_1}{n_1 c} d_{eff,1} E_1^*(Z) E_2(Z) e^{-i\Delta KZ} \quad (2)$$

$$\frac{dE_2(Z)}{dZ} = \frac{-i\omega_2}{n_2 c} d_{eff,2} E_1^2(Z) e^{+i\Delta KZ} \quad (3)$$

where the subscript 1 refers to the fundamental frequency, 2 refers to the second harmonic, and

$$\Delta K = 2K_1 - K_2 = \text{phase mismatch}$$

$$K = \frac{n\omega}{c} = \frac{2\pi n}{\lambda}$$

Assuming negligible depletion of the fundamental, Eq. 3 can be readily integrated to yield

$$P_2 = \frac{8\pi^2 d_{\text{eff}}^2}{n_1 n_2^2 \lambda_1^2} \sqrt{\frac{\mu_0}{\epsilon_0}} Z^2 \frac{P_1^2}{A} \left[ \frac{\sin(Z\Delta K/2)}{Z\Delta K/2} \right]^2 \quad (4)$$

The term in brackets in Equation 4 will normally cause the second harmonic power to vary sinusoidally with increasing crystal length and, thus, limit second harmonic power to a low value. This term arises from the fact that, in general, the indices of refraction of the crystal will be different for the fundamental and second harmonic wavelengths. Therefore, the second harmonic wave generated at some distance  $Z_1$  will not necessarily be in phase with the wave generated at  $Z_2$ , and destructive interference will occur.

In birefringent materials, the index of refraction depends on whether the wave is ordinary or extraordinary. One can take advantage of this property by polarizing the input (fundamental) beam with respect to the optical axis of the crystal in such a way as to cause both the fundamental and second harmonic waves to propagate with the same velocity (i.e.,  $\Delta K = 0$ ).

One way to achieve the phase match condition is to orient the birefringent crystal so that the indices of refraction at the fundamental and second harmonic frequencies are the same (Type I phase matching). For a negative uniaxial crystal (one in which  $n^e < n^0$  and the two nonoptic axes have the same dispersion curve), the condition which must be satisfied for phase match to occur is:

$$\theta_m = \sin^{-1} \left[ \frac{n_2^e}{n_1^0} \sqrt{\frac{(n_2^0)^2 - (n_1^0)^2}{(n_2^0)^2 - (n_2^e)^2}} \right] \quad (5)$$

where the superscript o refers to the ordinary wave, e to the extraordinary wave, and the phase match angle ( $\theta_m$ ) is the angle between the fundamental beam plane of polarization and the crystal optic axis.

Equation 4 can be rewritten to include the effects of phase match:

$$P_2 = \frac{8\pi^2 d_{\text{eff}}^2}{(n_1^0)^3 \lambda_1^2} \sqrt{\frac{\mu_0}{\epsilon_0}} z^2 \frac{P_1^2}{A} \quad (6)$$

where  $d_{\text{eff}} = \alpha x_2$ , and  $\alpha$  is a function of the phase match angle and the symmetry class of the particular crystal. For Type I phase matching,  $\alpha = \sin \theta_m$ . The conversion efficiency  $n = P_2/P_1$  can be easily obtained from Eq. 6.

Angle tuned phase matching is by no means easy. There are two parameters which determine how sensitive a particular crystal is to angular alignment. The first is beam acceptance angle, which is how far from the phase match angle an incident beam must be to produce  $4/\pi^2$  of the maximum second harmonic power (half-width of the phase-matching peak):

$$\Delta \theta = \frac{-\lambda_1 \Delta K}{2\pi (n_1^0)^3 \left[ (n_2^e)^{-2} - (n_2^0)^{-2} \right] \sin 2\theta_m} \quad (7)$$

The acceptance angle puts a limit on how much beam divergence is allowable and, hence, determines how tightly the beam can be focused; it also in general forces single mode operation.

The second criterion is beam walk-off, which defines when the extraordinary wave separates from the ordinary wave. The walk-off angle is given by

$$\delta = \tan^{-1} \left[ \frac{(n_1^0)^2}{2} \left( \frac{1}{(n_2^e)^2} - \frac{1}{(n_2^0)^2} \right) \sin 2\theta_m \right] \quad (8)$$

and arises from the fact that the Poynting vectors for the ordinary and extraordinary waves are diverging even though their propagation vectors are colinear. For a given beam size, the walk-off angle limits the useful crystal length since the generated beam no longer overlaps the fundamental beam.

The crystal used in this project was lithium iodate ( $\text{LiIO}_3$ ). This crystal was used mainly because it is thought to have the lowest absorption of any SHG crystals at the Iodine laser wavelength ( $1.315 \mu\text{m}$ ). The pertinent properties of  $\text{LiIO}_3$  are listed in Table I.

TABLE I. Properties of  $\text{LiIO}_3$  at  $1.315 \mu\text{m}^*$ .

$\chi_2$	$n_1^0$	$n_2^0$	$n_2^e$	$\theta_m$	$\Delta\theta$	$\delta$
$6.8 \text{ pm/V}$	1.8517	1.8790	1.7332	$24.3^\circ$	$0.3 \text{ mrad/cm}$	$3.65^\circ$

\*Private communication w/T. Nowicki, Interactive Radiation, Inc., Northvale, NJ.

## 3.0 EXPERIMENTAL RESULTS

## 3.1 Z-PINCH LASER

This project was started using a Z-pinch photolytic iodine laser which was built at the Air Force Weapons Laboratory (AFWL) (Ref. 9) (Fig. 1). It consisted of two concentric cylinders: the inner one was made of quartz and had an inner diameter of 57 mm, the outer one was made of Pyrex and had an inner diameter of 152 mm. The laser fuel ( $\text{CF}_3\text{I}$ ) and buffer gas (Ar) filled the inner cylinder; Xe gas filled the outer annulus. The cylinders were held in place by aluminum electrodes at either end. One of the electrodes was connected via low inductance coaxial cable to a 4320  $\mu\text{F}$  capacitor bank, which was typically charged to 5 kV. The other electrode was connected to ground. The current traveled through eight brass rods symmetrically located external to the cylinders to create a uniform magnetic field before it passed through the Xe. Brewster window mounts were attached to the outer face of both electrodes.

When the current from the capacitor bank flowed through the xenon, a plasma was created. The Xe plasma in turn optically pumped the  $\text{CF}_3\text{I}/\text{Ar}$  mixture, causing the  $\text{CF}_3\text{I}$  to dissociate into  $\text{CF}_3$  and  $\text{I}({}^2\text{P}_{1/2})$ , which emits at 1.315  $\mu\text{m}$ . Laser firing was achieved by applying a preionizing voltage ( $\sim 25$  kV) to the xenon. When operating properly, the Xe could hold off the 5 kV capacitor bank voltage indefinitely, but the low current 25 kV pulse applied to two aluminum strips placed at 180 deg on the outer perimeter of the outer cylinder caused the gas to instantaneously break down. Some typical oscilloscope traces are shown in Fig. 2. The voltage was measured at the hot electrode by a voltage divider network, and the current was measured by a Power Designs Model CVT-1A current transformer which encircled one of the brass rods. The IR pulse was monitored by an Opto-Electronics Ltd. Model GD10 germanium photodiode and a band-pass filter centered at 1315 nm. The visible (second harmonic) and ultraviolet (UV) (Xe flash) pulses were monitored by EG&G model FND100G silicon photodiodes. The band-pass filter used for the second harmonic wavelength had a center wavelength of 656 nm; the UV filter was centered at 267 nm to monitor the Xe flash output in the  $\text{CF}_3\text{I}$  absorption band. The laser was

operated using a stable resonator. The outcoupling mirrors used were 25% R or 50% R at 1.315  $\mu\text{m}$ . Laser performance depended critically on the cleanliness of the inner (quartz) tube and the Brewster windows. Periodically the quartz tube had to be cleaned with a 20 percent hydrofluoric (HF) acid solution to remove a milky film which formed on the outer surface of the tube. Under optimal conditions, the laser was superradiant. The beam shape was a strong function of pressure. At low total pressures, the beam was circular but it became increasingly annular as the pressure was increased (Fig. 3) because of the decreasing penetration depth of the pump light. The best laser output was found to occur at a  $\text{CF}_3\text{I}$  pressure of about 13.3 kPa (Fig. 4).

Extracavity SHG was performed with the Z-pinch laser. To prevent damage to the crystal, the laser output energy was decreased. This was not a simple matter. The constraints were: a) the pressure in the inner tube had to be maintained higher than the pressure in the outer tube to prevent the current from traveling through the center tube and fusing the metal parts together; and b) the pressure in the outer tube had to be high enough to hold off a 5 kV charge. Then the ratio of  $\text{CF}_3\text{I}/\text{Ar}$  had to be lowered until an acceptable flux was achieved, bearing in mind the crystal clear aperture ( $1 \times 1 \text{ cm}$ ). The result was a 2.7 kPa mixture of 10%  $\text{CF}_3\text{I}$  in Ar. The configuration used for extracavity SHG is shown in Fig. 5. The resulting oscilloscope traces are shown in Fig. 6a. Based on the response of the red detector (average value of 200 mV), the experimental conversion efficiency can be determined based on the IR calorimeter reading (0.6 J). The responsivity of the red photodiode was determined to be 0.62 V/W based on reflection losses between the SHG crystal and the photodiode, transmission line dividers, and photodiode quantum efficiency. Thus, a 200 mV photodiode response corresponds to  $0.2 \text{ V}/0.62 \text{ V/W} = 0.32 \text{ W}$  of second harmonic power. For a 40  $\mu\text{s}$  laser pulse, the average IR power is  $0.6 \text{ J}/40 \times 10^{-6} \text{ s} = 15 \text{ kW}$ . This corresponds to a conversion efficiency of  $2.1 \times 10^{-5}$ . To compare this number with the theoretical conversion efficiency  $\eta$  we begin by rearranging Eq. 6 to obtain

$$\eta = \frac{P_2}{P_1} = \frac{8\pi^2 d_{\text{eff}}^2}{(n_1^0)^3 \lambda_1^2} \sqrt{\frac{\mu_0}{\epsilon_0}} Z^2 \frac{P_1}{A} \quad (9)$$

Using  $d_{\text{eff}} = \chi_2 \sin \theta_m = 2.8 \text{ pm/V}$  (Table 1),  $\mu_0 = 1.26 \cdot 10^{-6} \text{ H/m}$ ,  $\epsilon_0 = 8.85 \cdot 10^{-12} \text{ F/m}$  and the value for  $n_1^0$  given in Table 1, Eq. 9 becomes

$$n = 2.12 \cdot 10^{-8} W \cdot Z^2 \cdot \frac{P_1}{A} \quad (10)$$

For the case at hand, the beam diameter = 1 cm,  $P_1 = 15 \text{ kW}$ , and  $Z = 1 \text{ cm}$ , so that  $n = 3.2 \cdot 10^{-4}$ . This order of magnitude discrepancy can be accounted for largely by beam divergence (half-angle = 3 mrad, which is an order of magnitude larger than the acceptance angle) and beam nonuniformity (Fig. 6b).

Attempts to perform intracavity SHG were severely complicated by the poor beam quality, high gain, and lack of reproducibility of the laser. To place the crystal intracavity, the beam size had to be decreased. This could be done by either an intracavity aperture or telescope. The use of an intracavity aperture necessitated low laser tube pressures due to the penetration depth effect. However, once the laser tube pressure (pure  $\text{CF}_3\text{I}$ ) was lowered below roughly 6.7 kPa to fill in the annulus, beam uniformity and output power reproducibility decreased significantly especially when the 1.2 cm aperture was placed intracavity. The other alternative, an intracavity telescope, required that the laser power be reduced to prevent crystal damage. Once again, irreproducible lasing, combined with the difficulty of aligning the telescope on a single shot laser made attempts at intracavity SHG futile.

### 3.2 ReCOIL LASER

Frequency doubling experiments were also conducted on ReCOIL, which is a chemical oxygen-iodine laser. The performance characteristics of COIL devices have been completely described elsewhere (Ref. 10) and are only briefly described here. ReCOIL is a chemical transfer laser in which excited oxygen ( $\text{O}_2^1\Delta$ ), produced by sparging chlorine through a mixture of basic hydrogen peroxide, is mixed with iodine molecules ( $\text{I}_2$ ). The resulting dissociation and excitation of iodine produces an inversion between the  $^2\text{P}_{1/2}$  and  $^2\text{P}_{3/2}$  states of atomic iodine, just as in the Z-pinch photolytic iodine laser described previously, with lasing at the  $1.315 \mu\text{m}$  wavelength.

The ReCOIL laser is a CW, relatively low (peak) power device. For this reason, extracavity frequency doubling was not pursued as it was with the Z-pinch laser; only intracavity frequency doubling was investigated.

The experimental setup for the ReCOIL doubling experiments is shown schematically in Fig. 7. The laser cavity consisted of a 100 percent reflecting at  $1.315 \mu\text{m}$  (max R) 5 m radius of curvature mirror and a flat 3 percent out-coupler separated by 1.5 m. Brewster windows on the ReCOIL device polarized the iodine radiation which maximized the efficiency of the doubling process. In addition, a 6 mm aperture was placed in the cavity since the diameter of the  $\text{LiIO}_3$  crystals was only 1 cm. As indicated in Fig. 7, both faces of the  $\text{LiIO}_3$  crystal had antireflection (AR) coatings for the  $1.315 \mu\text{m}$  wavelength which minimized the insertion loss within the resonator. The crystal itself was secured in a block which was attached to a combination of mounts. Together, the mounts had three rotational degrees of freedom as well as two translational degrees of freedom (perpendicular to the optic axis). In addition, a mechanical chopper was placed in the cavity since there was concern initially that an average power (which was too high) might damage the crystal or its AR coatings, although this proved to not be the case, even for run times of 25 s. For the same reason, no focusing elements were used, nor were higher reflectivity outcouplers tried.

Second harmonic powers were determined by taking advantage of the fact that the polarization of the second harmonic light is perpendicular to the polarization of the fundamental (iodine) radiation. Thus, the Brewster windows acted as an outcoupler for the second harmonic in accordance with the Fresnel equations (Ref. 11). A silvered reflecting mirror served to steer the second harmonic laser light through bandpass filters which ensured that only the second harmonic power reached the Newport Research Corporation power meter. Power meters were used to detect both second harmonic and fundamental powers, and a television camera recorded the meter displays in real time. Plexiglas sheets were used to make burn patterns of the outcoupled IR power. These burn patterns typically had areas of  $\approx 9 \text{ mm}^2$  which is considerably smaller than the iris  $28 \text{ mm}^2$  and suggested that at most a few modes were oscillating.

With a chopper duty cycle of 1/2, and no crystal inside the cavity, the out-coupled IR power was 10 W. With the insertion of the LiIO<sub>3</sub> crystal into the ReCOIL cavity, the total second harmonic power was calculated to be  $\approx$  60 mW (after correcting for the effect of the various filters), and the outcoupled IR power dropped to  $\approx$  7 W, suggesting that the crystal introduced some insertion loss into the cavity. Thus, the overall conversion efficiency was  $\approx$  1%. The conversion efficiency, however, was observed to depend critically on the alignment of the crystal.

Once again it is useful to compare the measured experimental power with that which is predicted by theory. The average red (second harmonic) power is equal to the average IR intracavity power times the single pass efficiency ( $\eta$ ) times 2, since the beam propagates in two directions:

$$\begin{array}{lcl} P_{\text{Avg.Red}} & = & P_{\text{Avg.IR Intracavity}} \cdot \eta \cdot 2 \\ & & \end{array} \quad (11)$$

To evaluate  $\eta$  (Eq. 10) for the experimental condition of interest, recall that the average outcoupled IR power was 7 W, but the peak outcoupled IR power must be 14 W since a chopper with a duty cycle of 1/2 was used. The peak intracavity power, on the other hand, is  $\approx$  33 times the outcoupled power since a 3 percent outcoupler was used. The crystal length was 1 cm (as discussed earlier) and the cross sectional area of the ReCOIL laser beam was 3 x 3 mm  $\approx$  0.09 cm<sup>2</sup>. Using Eq. 10, then, we have

$$\begin{aligned} \eta &= 2.12 \times 10^{-8} / W \cdot (1\text{cm})^2 \cdot (14W \cdot 33) / 0.09\text{cm}^2 \\ &= 1.09 \times 10^{-4} \end{aligned} \quad (12)$$

The predicted theoretical power is given by Eq. 11 and is

$$\begin{aligned} P_{\text{Avg. Red}} &= (7W \cdot 33) \cdot (1.09 \cdot 10^{-4}) \cdot 2 \\ &\approx 50 \text{ mW} \end{aligned} \quad (13)$$

which is lower than the measured output of  $\approx 60$  mW. Since the ReCOIL output consists of a few modes, however, the power is not uniform across the beam. Thus, the theoretical efficiencies should be higher than those calculated, and the theoretical and experimental values are in good agreement.

## 4.0 CONCLUSIONS

Frequency doubling experiments have been conducted with LiIO<sub>3</sub> crystals at the 1.315  $\mu\text{m}$  wavelength associated with the  $^2\text{P}_{1/2} \rightarrow ^2\text{P}_{3/2}$  transition of atomic iodine. Two different iodine lasers were used for this purpose. First, a photolytic iodine laser (Z-pinch) was used in experiments which concentrated on extracavity doubling. Typical frequency doubled outputs of 320 mW were observed in 40  $\mu\text{s}$  pulses at a conversion efficiency of  $2.1 \times 10^{-5}$ . In other experiments, a chemical oxygen iodine laser called ReCOIL was used in intra-cavity doubling experiments which produced 60 mW of average red power at an overall conversion efficiency of  $\approx 1\%$ . The conversion efficiencies in both experiments depended critically on the crystal's alignment. No damage to the crystal was observed, even at the typical (ReCOIL) average power fluxes of 5  $\text{kW/cm}^2$ . In both sets of experiments, calculated (theoretical) second harmonic powers were in good qualitative agreement with the observed results.

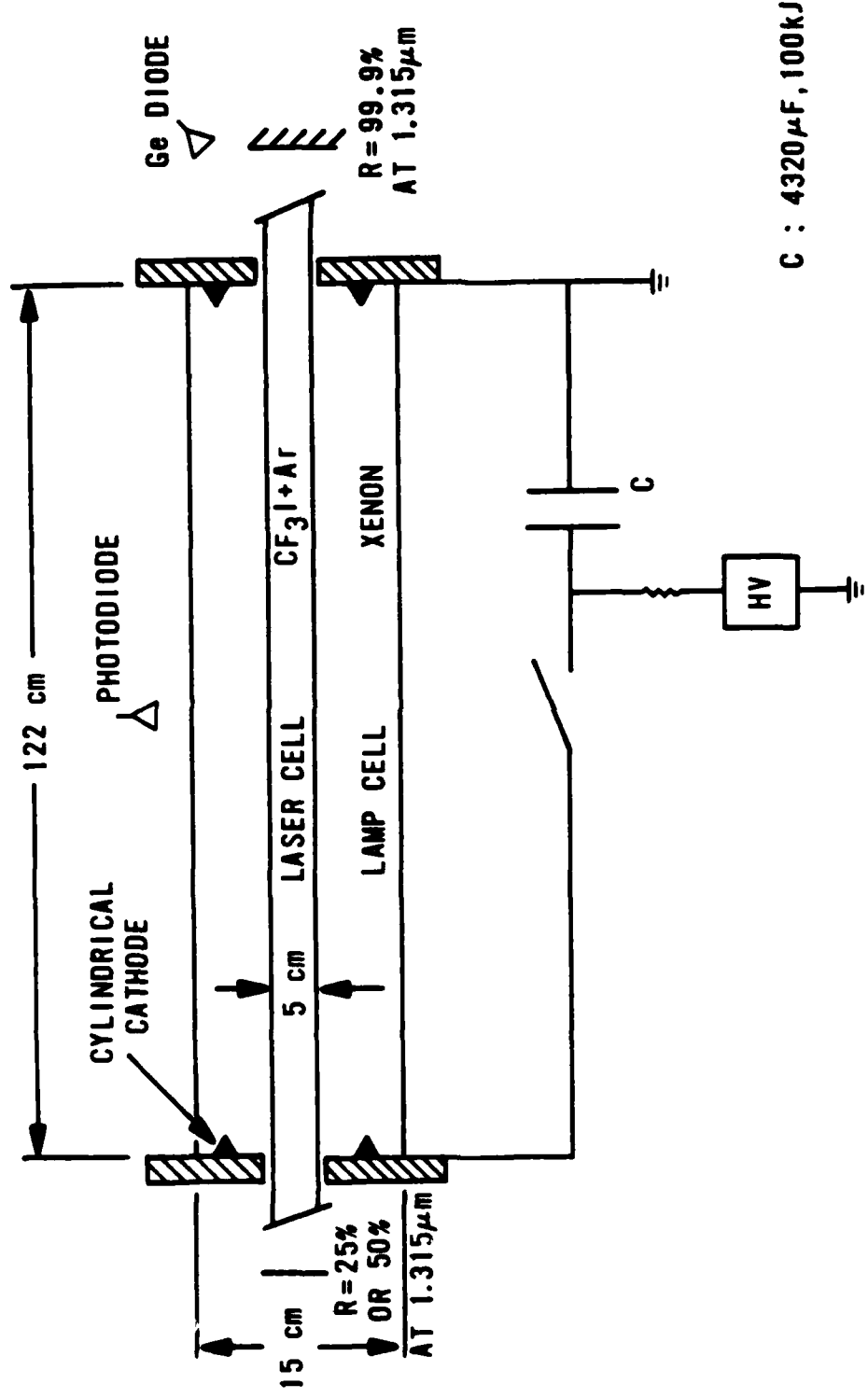
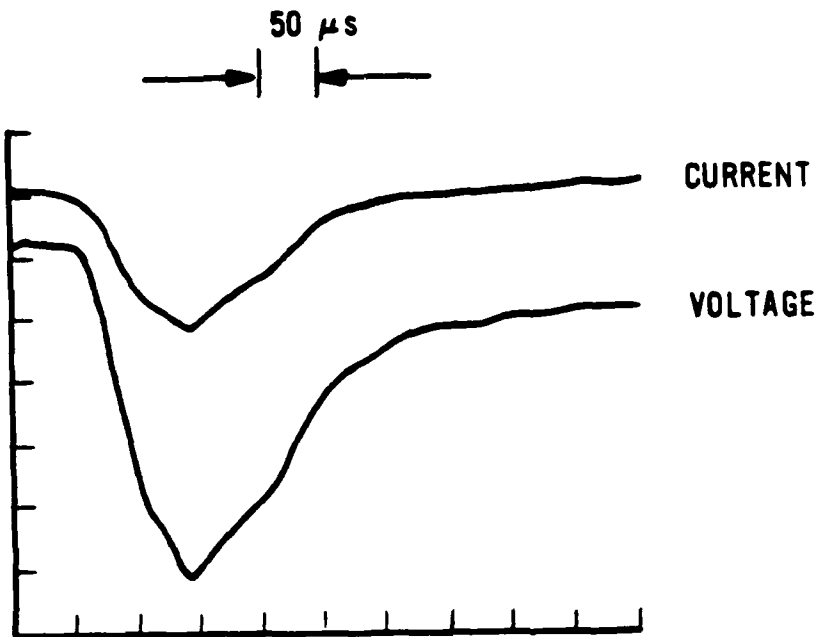
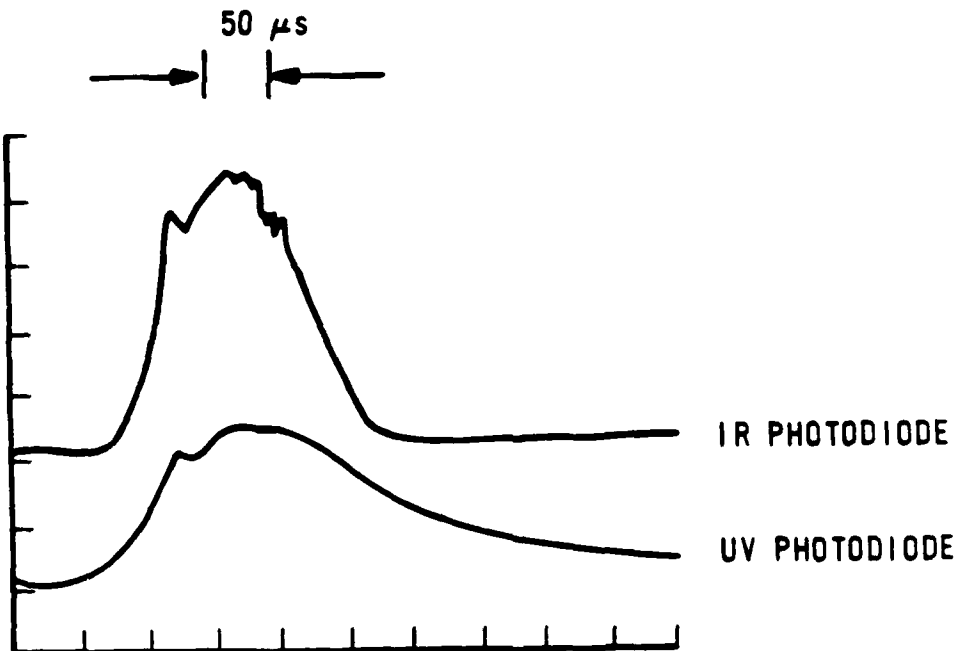


Figure 1. Schematic of the Z-pinch photolytic iodine laser.

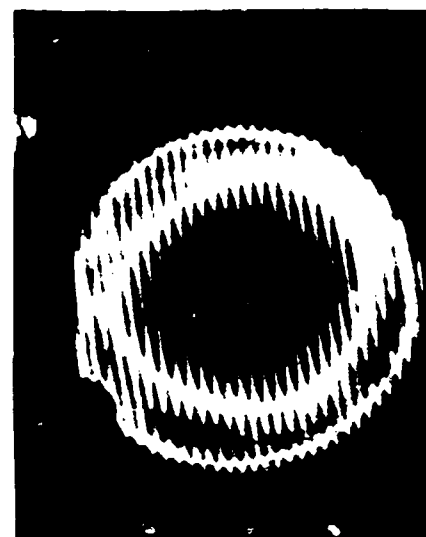


a. Typical current and voltage behavior of the discharge from the capacitor bank.



b. Temporal behavior of the xenon flash lamp output (UV) and the iodine laser (IR).

Figure 2. Oscilloscope traces.



(a)



(b)

Figure 3. Laser burn patterns made at (a) 50 torr  $CF_3I$  and (b) 200 torr  $CF_3I$ . The xenon pressure in both cases was 10 torr.

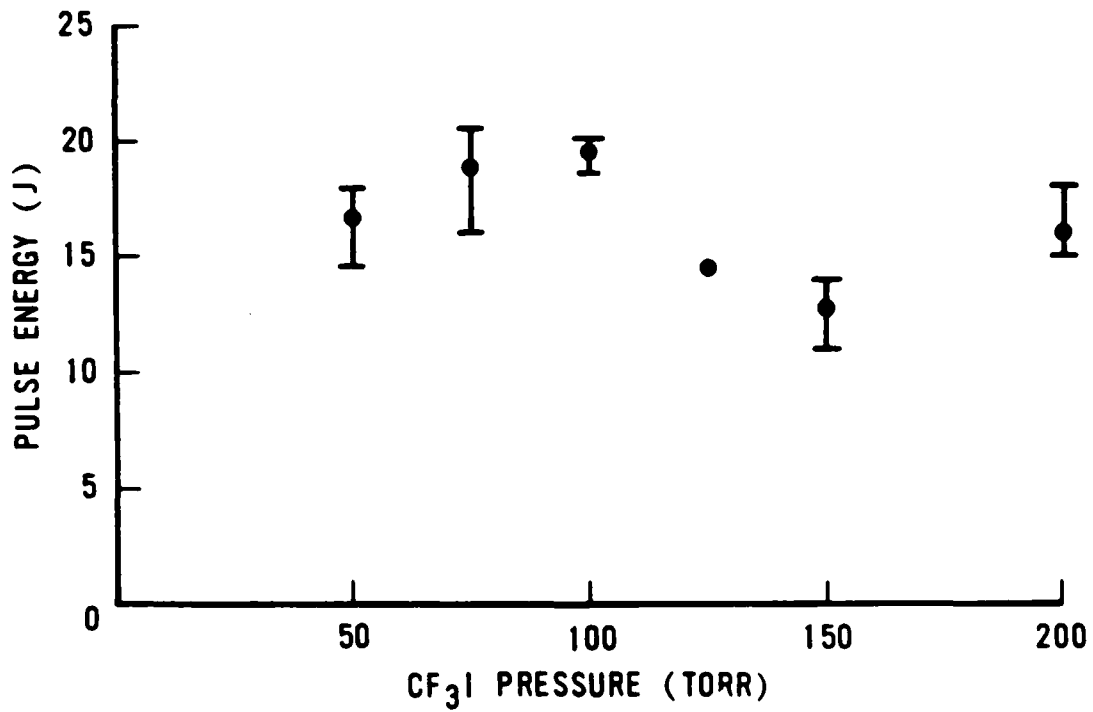


Figure 4. Laser pulse energy versus  $\text{CF}_3\text{I}$  pressure for a fixed xenon pressure of 10 torr. Maximum laser output was obtained at  $\approx 100$  torr (13.3 kPa). A measure of the spread in the data is indicated by error bars, and dots represent averages.

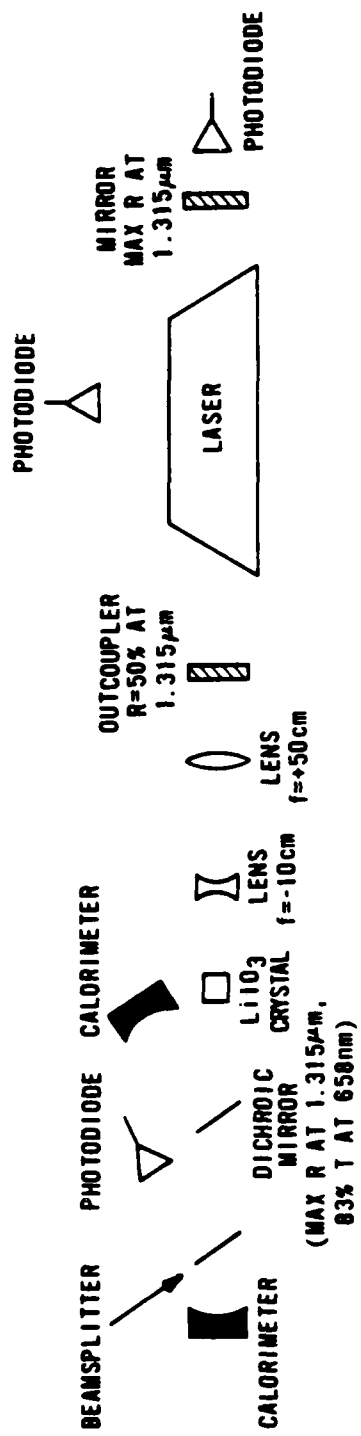
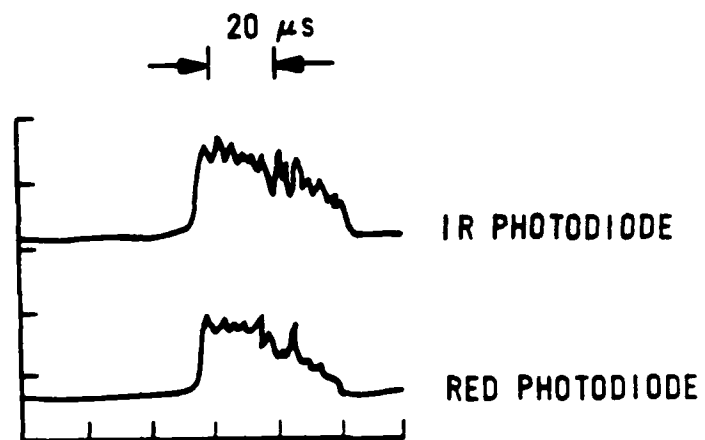


Figure 5. Schematic of the experimental setup used for frequency doubling of the photolytic iodine laser.



a. Temporal behavior of the fundamental (IR) and second harmonic (red) laser pulses.

 BURN PATTERN

b. Beam profile of the fundamental as it passed through the  $\text{LiIO}_3$  crystal (cf. Fig. 5).

Figure 6. Temporal and spatial laser outputs.

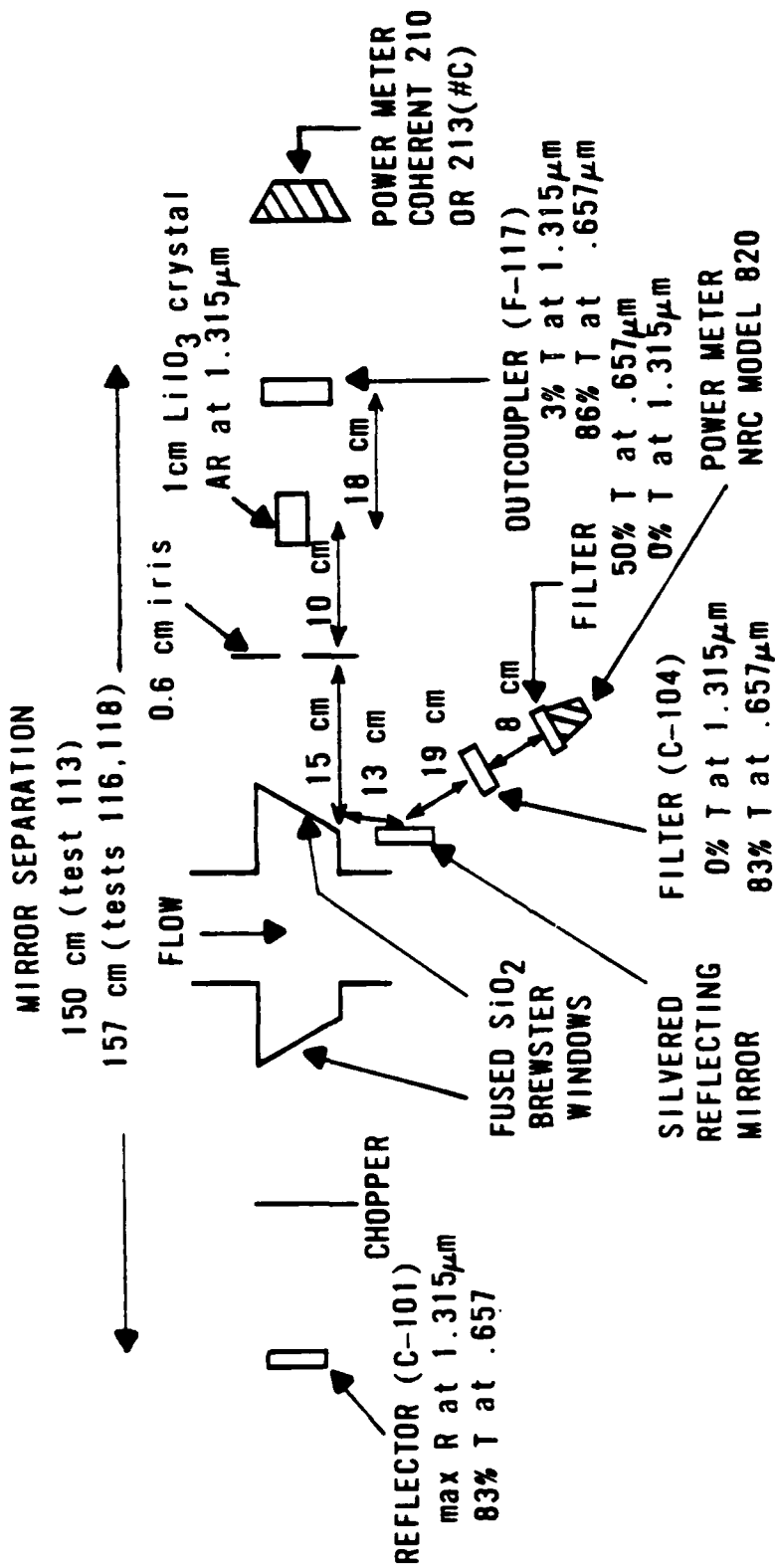


Figure 7. Schematic of the ReCOIL intracavity frequency doubling experiment.

## REFERENCES

1. Franken, P.A., Hill, A.S., Peters, C.W., and Weinreich, G., "Generation of Optical Harmonics," Phys. Rev. Letters, 7, p. 118 (1961).
2. Godwin, R.O. and Simmons, W.W., "How Industry Helped Build Nova, The World's Largest High-Precision Optical Project," Laser Focus, 21(4), p. 78 (1985).
3. Brederlow, G., Witte, K.J., Fill, E., Hohla, K. and Volk, R., "The Asterix III Pulsed High-Power Iodine Laser," IEEE J. Quant. Electr., QE-12(2), p. 152 (1976).
4. Smith, R.G., "Theory of Intracavity Optical Second-Harmonic Generation," IEEE J. Quant. Electr., QE-6(4), p. 215 (1970).
5. Geusic, J.E., Levinstein, H.J., Singh, S., Smith, R.G. and Van Uitert, L.G., "Continuous 0.532- $\mu$  Solid-State Source Using Ba<sub>2</sub>NaNb<sub>5</sub>O<sub>15</sub>," Appl. Phys. Lett., 12(9), p. 306 (1968).
6. Zernike, F. and Midwinter, J.E., Applied Nonlinear Optics (John Wiley Sons, New York, 1973).
7. Koechner, W. Solid-State Laser Engineering (Springer-Verlag, New York, 1976).
8. Yariv, A., Quantum Electronics (John Wiley and Sons, New York, 1975).
9. Stone, D.H., Saunders, D.P., and Clark, M.C., A Z-Pinch Photo-Pumped Pulsed Atomic Iodine Laser, AFWL-TR-83-33, Kirtland AFB, N. Mex., Mar 84.
10. Wiswall, C.E., Bragg, S.L., Reddy, K.V., Lilenfeld, H.V., and Kelly, J.D., "Moderate-Power CW Chemical Oxygen-Iodine Laser Capable of Long Duration Operation," J. Appl. Phys., 58(1), p. 115 (1985).
11. Hecht, E. and Zajac, A., Optics (Menlo Park, Calif., 1974)